




## Research Article

# Calculation of astrophysical reaction rate and uncertainty for $T(d,n)^4\text{He}$ using Bayesian statistical approach

Seyyed Soheil Esmaeili<sup>1</sup>, Abbas Ghasemizad<sup>1</sup> , and Omid Naserghodsi<sup>2</sup>

<sup>1</sup>Department of Physics, Faculty of Science, University of Guilan, Rasht, Guilan, Iran and <sup>2</sup>Department of Physics, Faculty of Science, University of Mazandaran, Babolsar, Mazandaran, Iran

### Abstract

One of the best methods to investigate and calculate a desired quantity using available limited data is the Bayesian statistical method, which has been recently entered the field of nuclear astrophysics and can be used to evaluate the astrophysical S-factors, the cross sections and, as a result, the nuclear reaction rates of Big Bang Nucleosynthesis. This study tries to calculate the astrophysical S-factor and the rate of reaction  $T(d,n)^4\text{He}$  as an important astrophysical reaction with the help of this method in energies lower than electron repulsive barrier, and for this purpose, it uses the R-Software, which leads to improved results in comparison with the non-Bayesian methods for the mentioned reaction rate.

**Keywords:** Bayesian statistics; Big Bang Nucleosynthesis; nuclear astrophysics; reaction rate

(Received 12 December 2023; revised 9 February 2024; accepted 20 February 2024)

### 1. Introduction

How is the Big Bang's correctness investigated?! Big Bang is based on three pillars: the Cosmic Microwave Background Radiation (CMBR or CMB), the universe inflation, and the Big Bang Nucleosynthesis (BBN), the first two of which have been proved both theoretically and experimentally. However, the third one has been faced with a serious problem. As one of the main branches of the nucleosynthesis theory in nuclear astrophysics, through studying the universe evolution using nuclear reactions, the BBN seeks to calculate the rates of the primary reactions of the very first moments of the Big Bang. Based on this theory, the Big Bang leads to the production of hydrogen (and its isotopes including deuterium and tritium), helium, and a little lithium through primary reactions network during the first 3 minutes of the universe life (Cowan et al. 2004; Coc 2016; Weinberg 1993). In this regard, the calculated values for the abundances of produced hydrogen, deuterium, and helium are in perfect agreement with the experimental measured values of the astrophysical observations. But the calculated value for the lithium abundance is three times (Iliadis et al. 2020) the experimentally measured value. This discrepancy is known as the *cosmological Lithium problem* in BBN. The explanations for the lithium problem include unknown systematic effects in  $^7\text{Li}$  observations, possible errors in thermonuclear reaction rates affecting the lithium and beryllium synthesis, physics beyond the standard model, and imprecise awareness of lithium developments in stars, despite the determined possible locations for each nuclei (Iliadis 2023).

**Corresponding author:** Abbas Ghasemizad; Email: [ghasemi@guilan.ac.ir](mailto:ghasemi@guilan.ac.ir)

**Cite this article:** Esmaeili SS, Ghasemizad A and Naserghodsi O. (2024) Calculation of astrophysical reaction rate and uncertainty for  $T(d,n)^4\text{He}$  using Bayesian statistical approach. *Publications of the Astronomical Society of Australia* 41, e019, 1–10. <https://doi.org/10.1017/pasa.2024.15>

However, it is believed that solving process of the lithium problem from the point of view of nuclear physics depends on the accurate calculation of the nucleosynthesis reaction rates related to the production or destruction of lithium and determining their exact abundances. Therefore, if the mentioned discrepancy is solved, the correctness of the BBN and then the Big Bang theory can be proved.

In this regard, many researches have been already focused on this problem and this field of research to calculate the exact value of reaction rates, such as Descouvemont et al. (2004) and Coc et al. (2015) using R-matrix and  $\chi^2$ -minimisation fits and Adelberger et al. (2011) for solar system. But lack of enough experimental data for some important reactions forces the researchers to use other methods compatible with the harsh situation of the lack of data that limits the possibility of accurate calculations. The new methods include Bayesian statistics that fits the mentioned harsh situation and will be explained in Section 3.

Therefore, in order to improve the mentioned discrepancy through exact calculating the S-factor and the reaction rates, this study investigates the S-factor and the reaction rate of  $T(d,n)^4\text{He}$  as a part of the BBN reactions network using a new method, and for this purpose, Bayes' principle and nuclear R-matrix theory are simultaneously used to infer an accurate output using available limited experimental data.

### 2. Importance of the $T(d,n)^4\text{He}$ reaction

Before this study, a number of studies had focused on the calculation of the rates of some reactions of the BBN reaction network (Fig. 1) using Bayesian method, such as  $d(p,\gamma)^3\text{He}$ ,  $^3\text{He}(^3\text{He},2p)^4\text{He}$  and  $^3\text{He}(\alpha,\gamma)^7\text{Be}$  (Iliadis et al. 2016),  $d(d,n)^3\text{He}$  and  $d(d,p)^3\text{H}$  (Iñesta, Iliadis, & Coc 2017),  $^3\text{He}(d,p)^4\text{He}$  (de Souza et al. 2019a),  $^7\text{Be}(n,p)^7\text{Li}$  (de Souza et al. 2020),  $^3\text{H}(d,n)^4\text{He}$

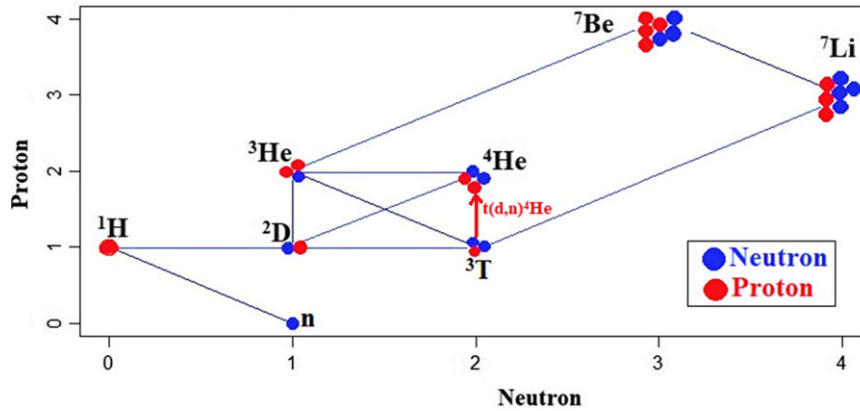


**Figure 1.** Big Bang Nucleosynthesis reaction network according to Nakamura et al. (2017). Each line represents a nuclear reaction.

(De Souza, Iliadis, & Coc 2019b),  $d(p,\gamma)^3\text{He}$  (Moscoso et al. 2021), and  $^{16}\text{O}(p,\gamma)^{17}\text{F}$  (Iliadis, Palanivelrajan, & de Souza 2022), all of which have been reviewed by (Esmaeili et al. 2022).

Among the BBN reactions network, the  $T(d,n)^4\text{He}$  reaction has been selected for this study, which has been marked with a red colour in Fig. 1.

The  $T(d,n)^4\text{He}$  reaction is considered as one of the most important reactions of the nuclear fusion for future terrestrial nuclear reactors because of its theoretical high nuclear gain of about 450–1 000. It is even considered and investigated as a space propulsion source or a power source (Chapman 2011) and also as a source of energy production in stars, which has the highest cross section and the amount of energy produced per reaction, which leads to the stable nucleus of  $^4\text{He}$ , and is also the basis of higher stages of fusion in older stars, hence one of the affecting factors on the lithium problem in BBN. This reaction is also considered as a possible source of intermediate energy ranged neutrons (Gagliardi et al. 1989) that can be used in different laboratories.

Because of its importance, as mentioned earlier, this reaction has been investigated by de Souza et al. (2019b), which resulted in better and improved S-factor and reaction rate, having lower calculation uncertainties. For the same reasons, this study tries to do the same investigation but with some different considerations in its performed method, which is described in the next section.

### 3. Method

In this study, Bayesian statistics is used as a new statistical method for nuclear calculations on the basis of limited available data, because it gives results with lower uncertainties in comparison with non-Bayesian methods (such as methods on the basis of  $\chi^2$ -minimisation). Bayes' principle (or Bayesian statistics) is used to fit the existing experimental data in order to further extrapolations. Bayes' principle in one of its applied forms can be expressed as follows:

$$P(\theta|y) = \frac{L(y|\theta) \cdot \pi(\theta)}{\int L(y|\theta) \cdot \pi(\theta) d\theta} \quad (1)$$

in which, the numerator expresses the product of the likelihood [ $L(y|\theta)$ ] (a postulated nuclear model) and the probability density of the priors [ $\pi(\theta)$ ] (primary form of the studied parameters in term of distribution functions), which gives the posterior [ $P(\theta|y)$ ]

(the updated distribution functions of the parameters as the output of the study) (de Souza et al. 2020). The denominator of the Equation (1) is a normalisation factor that has no special role in the calculations of this study and is considered as one, because the summation of all the possible probabilities is one. The likelihood in most of nuclear astrophysical calculations is defined as a product of the used distribution function for the astrophysical S-factor and the statistical uncertainty. This form of statistics uses a very scant experimental data of a phenomenon in order to estimate the best treat for that phenomenon.

All the basic considered parameters of the used model (likelihood) in this study are based on the nuclear R-matrix theory. According to previous studies in this field, the S-factor, as an astrophysical replacement for nuclear cross section, in single-level two-channel R-matrix theory can be written as:

$$S(E) = S_{bare}(E) \cdot \exp\left(\pi\eta \frac{U_e}{E}\right) \quad (2)$$

$$2\pi\eta = 0.98951013Z_0Z_1\sqrt{\frac{M_0M_1}{M_0+M_1} \frac{1}{E}} \quad (3)$$

where  $S_{bare}$  is for a nucleus without electron screening effect,  $2\pi\eta$  is the Sommerfeld parameter, and  $U_e$  is the electron screening potential (Iliadis 2015). Based on Baye et al. (2000), one can approximate and expand the S-factor parameter using Taylor series (expansion) as follows:

$$S_{bare}(E) = S(0) + S'(0)E + \frac{1}{2}S''(0)E^2 \quad (4)$$

in which, to calculate the  $S_{bare}$  using R-matrix theory, the following nuclear relation is considered:

$$S_{bare}(E) = E \cdot \exp(2\pi\eta) \cdot \sigma_{dn}(E) \quad (5)$$

in which, the reaction cross section ( $\sigma_{dn}$ ) is

$$\sigma_{dn}(E) = \frac{\pi}{k_d^2} \frac{2J+1}{(2J_1+1)(2J_2+1)} |S_{dn}|^2 \quad (6)$$

where  $k_d$  is the deuteron (projectile) wave number,  $J_1=1/2$  and  $J_2=1$  are the spins of the T (or  $^3\text{H}$ ) and deuteron ground state, respectively, with ( $J=3/2$ ) in this study, and  $S_{dn}$  is the scattering matrix element as follows:

$$|S_{dn}|^2 = \frac{\Gamma_d \Gamma_n}{(E_0 + \Delta - E_r)^2 + (\Gamma/2)^2} \tag{7}$$

where  $\Gamma_d$  and  $\Gamma_n$  are, respectively, the partial widths of the input channel  ${}^3\text{H} + d$  and the output channel  ${}^4\text{He} + n$ ,  $\Gamma$  is the total width,  $\Delta$  is the level shift,  $E_0$  is eigenvalue of energy, and  $E_r$  is the resonance energy of the studied reaction. The partial and total widths, and the level shift follow the below equations, respectively:

$$\Gamma = \sum_c \Gamma_c, \quad \Gamma_c = 2\gamma_c^2 P_c \tag{8}$$

$$\Delta = \sum_c \Delta_c = \Delta_1 + \Delta_2, \tag{9}$$

$$\Delta_c = -\gamma_c^2 (S_c - B_c)$$

where  $\gamma_c^2$  is the reduced width,  $B_c$  is the boundary condition parameter, and the energy-dependent quantities  $P_c$  and  $S_c$  are, respectively, the penetration factor and shift factor for channel  $c$  of a reaction (each of the two allowed reaction channels in this study) as:

$$P_c = \frac{k_d a_c}{F_\ell^2 + G_\ell^2},$$

$$S_c = \frac{k_d a_c (F_\ell F'_\ell + G_\ell G'_\ell)}{F_\ell^2 + G_\ell^2} \tag{10}$$

in which  $\ell$  is the orbital angular momentum of the reaction channel. The other useful parameter in R-matrix theory is  $a_c$  as the radius of the reaction channel:

$$a_c = r_0 \left( A_1^{\frac{1}{3}} + A_2^{\frac{1}{3}} \right) \tag{11}$$

where  $A_1$  and  $A_2$  are the mass numbers of two interacting nuclei (here, T and D), and  $r_0$  is a constant number between 1 and 2 fm.

The above-mentioned parameters are introduced in the Bayesian model of this study as the fitting parameters in the forms of probability density functions (PDF), which finally will result in the extrapolated S-factor distribution.

At the end, by numerical integration of reaction rate Equation (12), using the resulted S-factor, the reaction rates of T(d,n)<sup>4</sup>He are calculated for temperatures in the range of 1 MK to 10 GK:

$$N_A \sigma v = \left( \frac{8}{\pi m_{01}} \right)^{\frac{1}{2}} \frac{N_A}{(kT)^{\frac{3}{2}}} * \int_0^\infty S(E) \cdot \exp(-2\pi\eta) \exp\left(-\frac{E}{kT}\right) dE \tag{12}$$

where  $m_{01}$  is the reduced mass of the target and projectile, and  $kT$  is in term of MeV, which corresponds to Giga Kelvin temperatures.

However, the defined model in R-software for Bayesian analysis includes two types of parameters: *physical parameters* (resonance energy, reduced widths, and channel radii) and *experimental parameters* (data uncertainty and normalisation coefficients). Of course, in the end, only the S-factor is reported as the final goal of this study. Same as de Souza et al. (2020), in this study, the defined normal probability densities related to the priors of the physical parameters are truncated at zero (to not being negative). The considered priors are specified in Table 1 ( $\gamma_{WL}^2 \approx \frac{\hbar}{\mu \cdot a^2}$  is the Wigner limit with reduced mass  $\mu$  of the interacting components, Bohr radius  $a$ , and Planck constant  $\hbar$ ).

The calculating Markov chain of this study is based on a Metropolis–Hastings algorithm, and the model used to calculate

**Table 1.** The priors of the Bayesian model of this study.

Parameter	Prior
$E_0$	Uniform (0.02, 0.08)
$E_B$	TruncNormal (0, 1.0 <sup>2</sup> )
$\gamma_d^2$	TruncNormal $\left[ 0, \left( \gamma_{WL,d}^2 \right)^2 \right]$
$\gamma_n^2$	TruncNormal $\left[ 0, \left( \gamma_{WL,n}^2 \right)^2 \right]$
$a_d$	Uniform (2.5, 10.0)
$a_p$	Uniform (2.5, 10.0)
$U_c$	TruncNormal (0, 0.01 <sup>2</sup> )
$\sigma_{extr}$	TruncNormal (0, 5 <sup>2</sup> )
$\xi$	Lognormal (0, $\sigma_\xi^2$ )

the S-factor has the following nested form that contrary to de Souza et al. (2019b) and has four chains with the length of 50 000 and Burn-in of 1 000:

$$S'_i \sim Normal(S_i, \sigma_{extr,i}^2) \tag{13}$$

$$S''_{i,j} = f_{s,j} \times S'_i \tag{14}$$

$$S_{i,j}^{exp} \sim Normal(S''_{i,j}, \sigma_{Stat,i}^2) \tag{15}$$

where  $S_i$  is the experimental data of the S-factor,  $f_s$  is the statistical scaling factor, and  $\sigma$  represents the mentioned uncertainties of the calculations. For the scaling factor ( $f_s$ ), which is a number close to 1, the non-informative prior function was introduced with the form of the normal PDF, which has a mean value of 0 and a standard deviation of 100, and was again truncated at 0 to be positive. The indices ‘*extr*’ stand for the total unknown sources of the uncertainties, including statistical uncertainty and systematic uncertainty.

Furthermore, the experimental data points that were used as the input data into the defined model, along with the results of the defined model of this study for data extrapolation, will be mentioned later in the next section.

#### 4. Results and discussion

At first, it must be mentioned that, since all experiments are faced with uncertainties, which are divided into two *Statistical* and *Systematic* uncertainties, we have a reaction rate or equivalently the astrophysical S-factor as  $S_{\pm stat, \pm sys}^{\pm stat}$ , with  $\pm stat$  and  $\pm sys$  showing the statistical and systematic uncertainties, respectively.

There are a few data for S-factor in some limited areas of energy. In this study, all of the available datasets for the reaction are simultaneously used to find the curve of the studied quantity and also to estimate the value of S-factor in the missed areas using statistical fitting methods, such as extrapolations that are based on Bayesian principal. It must be emphasised that the mentioned data points are all of the available valid data that are based on experiments. However, to analyse the behaviour of the astrophysical S-factor (equivalent to the cross section) of the deuterium-tritium reaction, T(d,n)<sup>4</sup>He, in the low-energy regions, the data of Jarmie et al. (1984), Brown, Jarmie, & Hale (1987), Kobzev et al. (1966), Arnold et al. (1954), and Conner, Bonner, & Smith (1952) (see Appendix A) were used in our Bayesian model

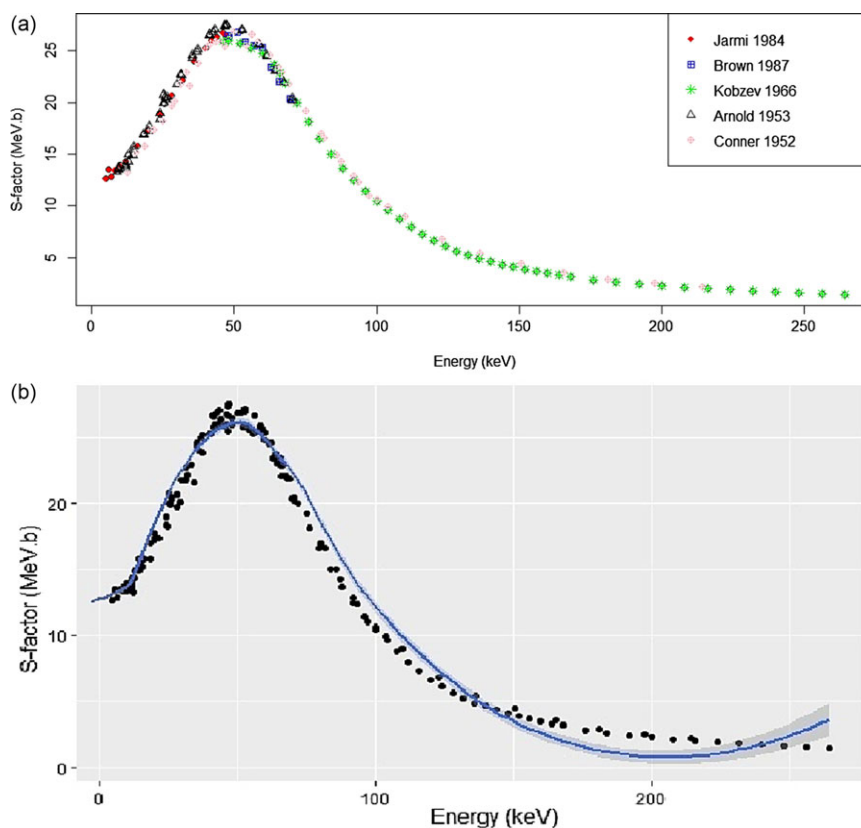


**Figure 2.** The astrophysical S-factor (equivalent to the cross section) for T(d,n)<sup>4</sup>He. Panel (a) shows the distribution of the data points, and the panel (b) shows the Bayesian fit for the data points as a blue line, and the grey credible interval.

mentioned in Section 3, which resulted in Fig. 2 as the data fit for the astrophysical S-factor.

As can be seen, the behaviour of the S-factor at low energies is dominated by a broad resonance at an energy lower than 50 keV, and as the energy decreases, its value also drops to about 12 MeV.b.

However, after the final fitting process, the value of  $S_{bare-0} = 12.11^{+0.089}_{-0.091}$  MeV.b was obtained that found to be in very good agreement with the results of de Souza et al. (2019b) in their Fig. 3, with a very slight difference: the uncertainty value in this study is slightly higher than those of de Souza et al. (2019b). Also, in comparison, for example, with  $S_{0.04} = 25.87 \pm 0.49$  MeV.b from Bosch et al. (1992), which obviously represents higher uncertainties, the results of the Bayesian method yields lower uncertainties, hence a better result. It should be noted that the value reported by de Souza et al. (2019b) for the S-factor is not for zero energy ( $\neq S_0$ ), but instead, for the value of S-factor in energies about 0.04 ( $S_{0.04} = 25.438^{+0.080}_{-0.089}$  MeV.b), which is again in very close agreement with the value obtained in the diagram of Fig. 2 of this study. Regarding this difference between the reported S-factors for different energy regions, the reported S-factors of the two studies just *apparently* seem to be different, but in fact, they are not, since the S-factor on the 0.04 MeV in this study is  $S_{0.04} = 25.518^{+0.085}_{-0.088}$  MeV.b, which is closely similar to the one reported by de Souza et al. (2019b) at the same energy.

Furthermore, for the electron screening effect, as can be seen in Fig. 2 as the astrophysical S-factor variation diagram, at very low energies (less than 10 keV), no significant electron screening

effect can be expressed for this reaction, and only a limit can be considered, which of course will have a small value (about only a few eV), and for this reason, the S-factor diagram does not increase at very low energies under the influence of this effect and does not goes up but instead is stopped at a certain value. The result of this study as the non-significant electron screening effect for the T(d,n)<sup>4</sup>He reaction is in full agreement with the result of de Souza et al. (2019b), while this result disagree with the reports of some studies, including Langanke et al. (1989). The agreement between the results of this study and those of de Souza et al. (2019b) shows that choosing a higher number of Markov chains with different length and Burn-in does not make significant differences on the final results.

Moreover, from the diagram of Fig. 2, it can be seen that the data of Kobzev et al (1966) in the sequence of higher energies describes the behaviour of the S-factor better than those of Kobzev et al. (1966) and also Arnold et al. (1954), whose data provide a better description of the S-factor in low energies, while the study of Conner et al. (1952) describes the variations of the S-factor very well in both high- and low-energy regions.

At the end, using the resulted S-factor ( $S_{bare}$ ), and after replacing it in the reaction rate formula (Equation (12)), the reaction rate values can be calculated for a range of temperatures, whose output graph is as Fig. 3 indicates.

The reaction rate curve has been plotted by numerical integration of Equation (12) using the same S-factor ( $S_{bare}$ ) of the previous section (calculated using the Bayesian model) and considering

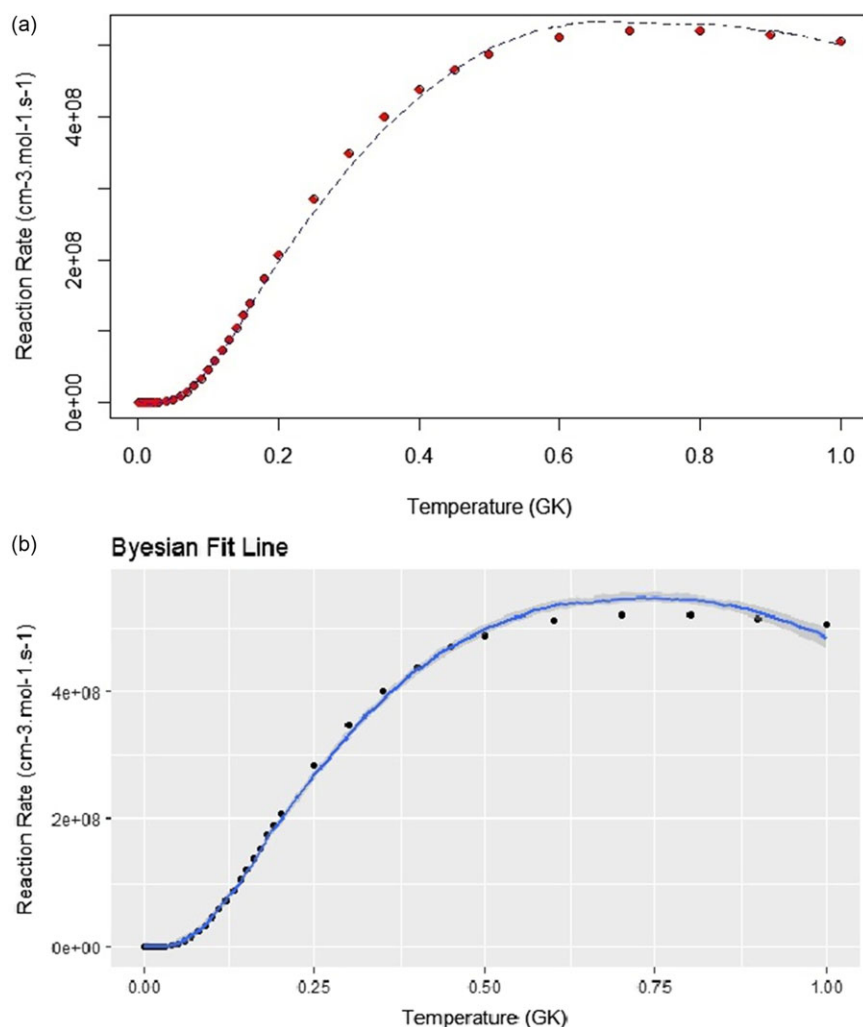


**Figure 3.** Reaction rate at GK for  $T(d,n)^4\text{He}$ . Panel (a) shows the distribution of the reaction rate data points, and the panel (b) shows the Bayesian fit for them as a blue line, and the grey credible interval.

the 50<sup>th</sup> percentiles of the deduced probability densities. These values can be found in Appendix B.

It can be seen in Fig. 3 that with the increase in the temperature, since the kinetic energy of the interacting particles increases, conditioned by enough or high abundances of deuterium and tritium in the environment, the reaction rate grows until it reaches a limit of about  $5 \times 10^8 \text{ cm}^{-3} \text{ mol}^{-1} \text{ s}^{-1}$ . Of course, further growth of the reaction rate is possible and is not limited to the mentioned value, but the conditions and temperature of the environment (the energy of the interacting particles) play vital roles in the occurrence of the reaction. At the lower temperatures (energies), due to the energy decrease of the interacting particles (deuterium and tritium), which are less able to penetrate the Coulomb repulsive barrier, the reaction rate undergoes a sharp exponential decrease and gives a value close to zero, which can be seen in the diagram, but this reduction of the rate to zero is actually due to the insignificant rate of the reaction, and in practice, it does not exactly mean as the complete cessation of the reaction in the star environment.

The exponential curve of Fig. 3 is an estimate of the likely behaviour of the reaction rate function with respect to

temperature. As mentioned, the changes of the reaction rate of  $T(d,n)^4\text{He}$  can be considered as relatively exponential.

Reconsidering the changes of the temperature, the energy and the resulted astrophysical S-factor for the d-t reaction in terms of each other obtains the following contour plots of Figs. 4 and 5.

In the graph of Fig. 4, the blue area shows the lowest S-factors, while the red area shows the highest values of the S-factor in terms of temperature and energy. As can be seen in the contour plot of Fig. 4, the value of the S-factor at an energy of about 50 keV and a temperature of about 5.8 K has a maximum value, which is actually the resonance of the cross section of the reaction in the mentioned energy (temperature) region. But in the areas around it, the S-factor decreases, which is a good representation of the resonant behaviour of the cross section of the studied reaction in this energy range; hence a proof that the studied reaction has a resonant behaviour in this region.

Also, the presence of S-factor values can be seen only in the upper regions of above the line  $E=a_1T$ . It should be noted that the energy and temperature of the stellar environment, where the reactions take place, are actually equivalent concepts in nuclear

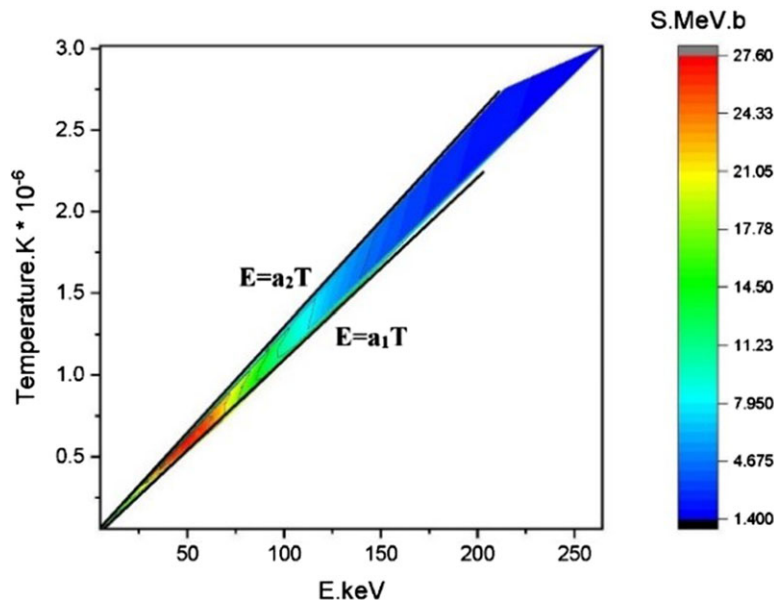


**Figure 4.** Astrophysical S-factor (MeV.b) contour plot as a quantity for reaction rate in terms of temperature (Kelvin) and energy (keV) for the  $T(d,n)^4\text{He}$  reaction.

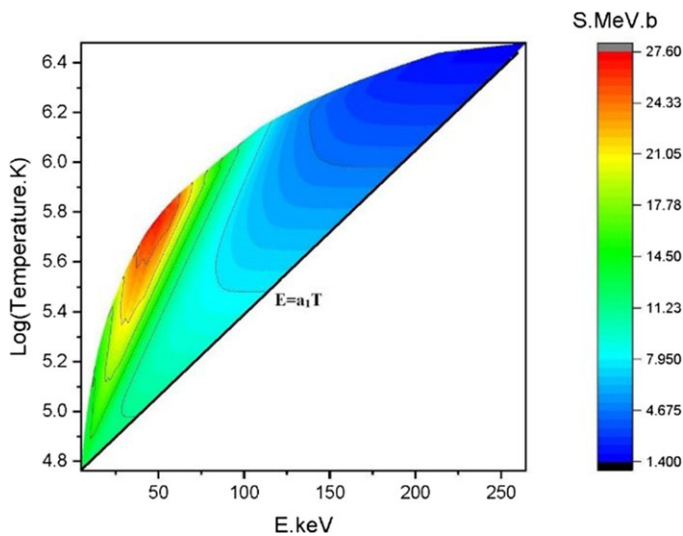


**Figure 5.** Astrophysical S-factor (MeV.b) contour plot as a quantity for reaction rate in terms of logarithmic temperature (Kelvin) and energy (keV) for the  $T(d,n)^4\text{He}$  reaction.

physics, hence linearly dependent on each other with a coefficient as  $a_1$ . As a result, the linear dependence of these two quantities can be seen as black diagonal lines having the slope of  $a_1$  and  $a_2$ . Naturally, in the area below the line  $E=a_1T$ , the S-factor does not have any values, because in this area, temperature and energy are not of the same nature; hence, a specific cross section cannot be obtained in this circumstance. The slope  $a_1$  indicating the dependence between the two quantities of energy and temperature as  $E=a_1T$  is the conversion coefficient between two mentioned quantities in nuclear physics ( $a_1=11\,600\text{ eV}/300\text{ K}=38.67\text{ eV K}^{-1}$ ).

It is also noteworthy that the value of the S-factor will be limited to a certain upper limit. Therefore, according to the diagram, the

value of S-factor will be between the two border regions of  $E=a_1T$  and  $E=a_2T$ . The slope of the upper boundary line ( $a_2$ ) will depend on the value of different values of the S-factor, because especially for some energy and temperature values, several close cross sections (S-factor) are obtained from different studies. As a result, the resulting contour plot will have two boundaries (or a hill-top point in its 3D view).

In the diagram of Fig. 5, where the temperature has been plotted logarithmically, again the S-factor is maximised in the energy of about 50 keV and the logarithmic temperature equal to about 0.58 (with the corresponding unit), showing the same resonance that was mentioned before, and having the same dependence line of energy and temperature as  $E=a_1T$  ( $a_1=11\,600\text{ eV}/300\text{ K}=38.67\text{ eV K}^{-1}$ ).

The importance of the two diagrams of Figs. 4 and 5 is that the simultaneous dependence of the astrophysical S-factor on both energy and temperature quantities can be seen, and at the same time, the resonance in the cross section of the reaction is well evident.

However, as a comparison with this study, the model used by de Souza et al. (2019b) had three longer chains, while the model of this study uses four shorter chains instead, to investigate the calculation independency of the number and length of the chains. It must be mentioned that the whole other studies in this field, such as Iliadis et al. (2016), de Souza et al. (2019a), (2020), Moscoso et al. (2021), and Iliadis et al. (2022) have used three chains for their calculations.

Furthermore, this study mainly uses *dnorm* and *dunif* functions for its defined models so as to consider a normal distributions for the input data, which makes no significant difference on the final results in comparison with other studies, such as de Souza et al. (2019b).

However, according to the numerical values obtained for the studied reaction (increase in the cross section and as a result, the increase in the reaction rate of  $T(d,n)^4\text{H}$ ), and by referring to Fig. 1, it can be seen that this increase will require more deuteron

consumption; therefore, the amount of the conversion of these two nuclei into lithium will reduce to a negligible extent, which confirms the reduction of the discrepancy between the theoretical and experimental values of lithium abundances, hence leading to an improvement in lithium problem. But due to the slight decrease of this value, it cannot be claimed that the existing problem has been completely resolved, but only an insignificant reduction (in the range of only a few percent compared to the difference of three times between the theoretical and experimental values) will be resulted, and the lithium problem will still remain, the reason for which should be in other cases, including a correction on the Big Bang theory.

## 5. Conclusion

In this study, using the R-program (R Core team 2015), four short Markov chains using a Bayesian model (likelihood) having different components with different values and distribution functions in comparison with latest studies in this field were used in order to find the behaviour of the astrophysical S-factor and consequently the reaction rate for  $T(d,n)^4\text{He}$  as one of the most important reactions in nuclear astrophysics, playing a crucial role in BBN.

As the first result, making changes in the defined models and functions with different imported values and also changing the Markov chains made no significant difference in the final values of the S-factor or the studied reaction rate.

Also, as the second result of this study, despite the innovation and efficiency of Bayesian method, only little improvements have been made on the primary lithium abundances. Therefore, to justify this condition and the inadequacy of the models used so far to solve the lithium problem, this interpretation can be proposed that these kinds of calculations have no significant impact on the abundance of lithium, and as a result, the reason for the discrepancy between the theoretical and experimental values of the initial abundance of lithium should be explained using other considerations, including a new correct knowledge of the lithium destruction mechanism in proto-stars or the need for a new related physics theory, especially correcting the Big Bang theory in some of its aspects, such as BBN development process, star evolution process, or so on.

Therefore, despite the correctness and effectiveness of the current calculations, the need to complete such calculations is still remained and other factors should and can be included in to fully solve the lithium problem.

**Competing interest.** The authors declare that they have no known competing financial interests or personal relationships that could have appeared to influence the work reported in this paper.

**Data Availability.** Not applicable.

## References

- Adelberger, E. G. 2011, *RvMPh*, 83, 195.  
 Arnold, W. R., Phillips, J. A., Sawyer, G. A., Stovall, Jr. E. J., & Tuck, J. L. 1954, *PhRv*, 93, 483.  
 Baye, D., & Brainin, E. 2000, *PhRvC*, 61, 025801.  
 Brown, R. E., Jarmie, N., & Hale, G. M. 1987, *PhRvC*, 35, 1999.  
 Bosch, H. S., & Hale, G. M. 1992, *NF*, 32, 611.

- Chapman, J. J. 2011, in 38th International Conference on Plasma Science (ICOPS) (No. NF1676L-12188). <https://doi.org/10.1109/PLASMA.2011.5992998>.  
 Coc, A., Petitjean, P., Uzan, J. P., Vangioni, E., Descouvemont, P., Iliadis, C., & Longland, R. 2015, *PhRvD*, 92, 123526.  
 Coc, A. 2016, *JPhCS*, 665, 012001. IOP Publishing.  
 Conner, J. P., Bonner, T. W., & Smith, J. R. 1952, *PhRv*, 88, 468.  
 Cowan, J. J., & Thielemann, F. K. 2004, *PhT*, 57, 47.  
 De Souza, R. S., Boston, S. R., Coc, A., & Iliadis, C. 2019a, *PhRvC*, 99, 014619.  
 De Souza, R. S., Iliadis, C., & Coc, A. 2019b, *ApJ*, 872, 75.  
 De Souza, R. S., Kiat, T. H., Coc, A., & Iliadis, C. 2020, *ApJ*, 894, 134.  
 Descouvemont, P., Adahchour, A., Angulo, C., Coc, A., & Vangioni-Flam, E. 2004, *ADNDT*, 88, 203.  
 Esmaeili, S. S., Ghasemizad, A., Naserghodsi, O., & Sendesi, S. M. T. 2022, *IJSTT*, 46, 1085.  
 Gagliardi, C. A., & Betker, A. C. 1989, *NIMPhRS*, 284, 356.  
 Iliadis, C., Anderson, K. S., Coc, A., Timmes, F. X., & Starrfield, S. 2016, *ApJ*, 831, 107.  
 Iliadis, C., & Coc, A. 2020, *ApJ*, 901, 127.  
 Iliadis, C. 2015, *Nuclear Physics of Stars* (John Wiley & Sons)  
 Iliadis, C., Palanivelrajan, V., & de Souza, R. S. 2022, *PhRvC*, 106, 055802.  
 Iliadis, C., & Website of Nuclear Astrophysics: <https://iliadis.web.unc.edu/big-bang-nucleosynthesis/>; Cited at June 2023.  
 Iñesta, Á. G., Iliadis, C., & Coc, A. 2017, *ApJ*, 849, 134.  
 Jarmie, N., Brown, R. E., & Hardekopf, R. A. 1984, *PhRvC*, 29, 2031.  
 Kobzev, A. P., Salatskij, V. I., & Telezhnikov, S. A. 1966, *SJNP*, 3, 774.  
 Langanke, K., & Rolfs, C. 1989, *MPhLA*, 4, 2101.  
 Moscoso, J., De Souza, R. S., Coc, A., & Iliadis, C. 2021, *ApJ*, 923, 49.  
 Nakamura, R., Hashimoto, M., Ichimasa, R., & Arai, K. 2017, *IJMPE*, 26, 1741003.  
 R Core Team, 2015, Vienna, Austria (<https://www.R-project.org/>).  
 Weinberg, S. 1993, *The First Three Minutes: A Modern View of the Origin of the Universe* (New York: Basic Books) [primera edición en castellano publicada por Alianza, Madrid, 1978]

## Appendix A. The data used for the $T(d,n)^4\text{He}$ reaction calculations

Reference	E (keV)	$\pm \Delta E_{\text{CM}}$		$\pm \Delta S_{\text{stat}}$		Systematic uncertainty
		(eV)	S (MeV.b)	(MeV.b)		
Jarmie et al. (1984)	4.992	2.4	12.63	0.58	0.0126	
	5.99	2.66	13.48	0.39	0.0126	
	6.99	2.92	12.83	0.4	0.0126	
	7.99	3.18	13.43	0.27	0.0126	
	9.989	3.44	13.92	0.14	0.0126	
	11.989	3.7	14.32	0.1	0.0126	
	15.99	3.96	15.81	0.13	0.0126	
	19.992	4.22	17.35	0.09	0.0126	
	23.994	4.48	18.87	0.08	0.0126	
	27.996	4.74	20.7	0.09	0.0126	
	31.998	5	22.19	0.11	0.0126	
	36.001	5.26	24.02	0.11	0.0126	
	40.004	5.52	25.28	0.14	0.0126	
	42.005	5.78	26	0.12	0.0126	
	44.007	6.04	26.3	0.14	0.0126	
46.009	6.3	26.74	0.13	0.0126		
46.809	6.4	26.64	0.14	0.0126		

Reference	E (keV)	$\pm \Delta E_{CM}$		$\pm \Delta S_{stat}$	Systematic uncertainty
		(eV)	S (MeV.b)	(MeV.b)	
Brown et al. (1987)	47.948	9	26.48	0.21	0.0126
	50.947	9	26.84	0.21	0.0126
	53.942	9	25.89	0.21	0.0126
	56.942	9	25.5	0.2	0.0126
	59.941	9	25.33	0.19	0.0126
	62.941	9	23.44	0.19	0.0126
	65.941	9	22.02	0.18	0.0126
	69.541	9	20.34	0.16	0.0126
Kobzev et al., (1966)	46	1.2	25.93	0.52	0.025
	48	1.2	25.96	0.52	0.025
	52	1.3	25.76	0.52	0.025
	56	1.4	25.28	0.51	0.025
	60	1.5	24.77	0.5	0.025
	64	1.3	23.66	0.47	0.025
	66	1.3	22.85	0.46	0.025
	68	1.4	21.89	0.44	0.025
	72	1.4	19.98	0.4	0.025
	76	1.5	18.14	0.36	0.025
	80	1.6	16.53	0.33	0.025
	84	1.7	15.01	0.3	0.025
	88	1.8	13.65	0.27	0.025
	92	1.8	12.5	0.25	0.025
	96	1.9	11.41	0.23	0.025
	100	2	10.45	0.21	0.025
	104	2.1	9.59	0.19	0.025
	108	2.2	8.76	0.18	0.025
	112	2.2	7.98	0.16	0.025
	116	2.3	7.28	0.15	0.025
120	2.4	6.65	0.13	0.025	
124	2.5	6.08	0.12	0.025	
128	2.6	5.61	0.11	0.025	
132	2.6	5.23	0.1	0.025	
136	2.7	4.89	0.1	0.025	
140	2.8	4.6	0.09	0.025	
144	2.9	4.32	0.09	0.025	
148	3	4.11	0.08	0.025	
152	3	3.88	0.08	0.025	
156	3.1	3.69	0.07	0.025	
160	3.2	3.5	0.07	0.025	
164	3.3	3.32	0.08	0.025	
168	3.4	3.15	0.08	0.025	
176	3.5	2.84	0.07	0.025	
184	3.7	2.62	0.07	0.025	
192	3.8	2.42	0.06	0.025	

Reference	E (keV)	$\pm \Delta E_{CM}$		$\pm \Delta S_{stat}$	Systematic uncertainty
		(eV)	S (MeV.b)	(MeV.b)	
	200	4	2.26	0.06	0.025
	208	4.2	2.13	0.05	0.025
	216	4.3	2	0.05	0.025
	224	4.5	1.89	0.05	0.025
	232	4.6	1.79	0.04	0.025
	240	4.8	1.69	0.04	0.025
	248.2	5	1.6	0.04	0.025
	256.2	5.1	1.51	0.04	0.025
	264.3	5.3	1.44	0.04	0.025
Arnold et al., (1954)	8.98	75	13.34	0.026	0.02
	9.32	75	13.703	0.027	0.02
	9.47	75	13.508	0.027	0.02
	9.52	75	13.6	0.027	0.02
	11.95	75	14.068	0.028	0.02
	11.99	75	13.849	0.028	0.02
	12.03	75	13.68	0.027	0.02
	12.81	75	14.302	0.029	0.02
	12.83	75	14.957	0.03	0.02
	14.48	75	14.939	0.03	0.02
	14.68	75	15.753	0.031	0.02
	14.89	75	15.448	0.03	0.02
	18.33	75	16.921	0.034	0.02
	18.35	75	16.989	0.032	0.02
	19.92	75	17.249	0.034	0.02
	20.27	75	17.721	0.035	0.02
	23.95	75	18.969	0.038	0.02
	23.97	75	18.366	0.036	0.02
25.17	75	20.718	0.021	0.02	
25.26	75	20.755	0.021	0.02	
25.32	75	19.969	0.02	0.02	
25.66	75	19.92	0.02	0.02	
25.72	75	20.596	0.02	0.02	
26.09	75	20.277	0.02	0.02	
26.38	75	20.525	0.02	0.02	
29.95	75	21.766	0.022	0.02	
31.16	75	22.749	0.023	0.02	
31.52	75	22.695	0.023	0.02	
35.36	75	24.314	0.024	0.02	
35.38	75	24.589	0.024	0.02	
37	75	24.967	0.025	0.02	
37.16	75	25.184	0.025	0.02	
41.23	75	26.6	0.027	0.02	
41.25	75	26.514	0.026	0.02	
43.29	75	27.067	0.027	0.02	
42.49	75	26.847	0.027	0.02	



Reference	E (keV)	$\pm \Delta E_{CM}$		$\pm \Delta S_{stat}$	Systematic uncertainty
		(eV)	S (MeV.b)	(MeV.b)	
	46.61	75	27.446	0.027	0.02
	46.64	75	27.365	0.027	0.02
	46.65	75	27.489	0.027	0.02
	47.22	75	27.505	0.027	0.02
	47.25	75	27.542	0.027	0.02
	52.8	75	26.975	0.027	0.02
	52.83	75	27.085	0.027	0.02
	58.66	75	25.621	0.025	0.02
	58.68	75	25.669	0.026	0.02
	61.39	75	24.593	0.024	0.02
	61.43	75	24.492	0.024	0.02
	64.51	75	23.071	0.023	0.02
	64.54	75	23.157	0.023	0.02
	67.37	75	22.002	0.022	0.02
	67.39	75	21.951	0.022	0.02
	70.39	75	20.445	0.02	0.02
	70.44	75	20.227	0.02	0.02
<hr/>					
Conner et al. (1952)	12.42	60	13.23	0.13	0.018
	15.48	73	15.17	0.15	0.018
	18.6	86	15.79	0.16	0.018
	20.7	99	17.33	0.17	0.018
	21.78	112	17.38	0.17	0.018
	24.9	125	18.23	0.18	0.018
	28.02	138	19.7	0.2	0.018
	29.1	151	20.13	0.2	0.018
	31.2	163	21.8	0.22	0.018
	33.24	175	22.91	0.23	0.018
	34.26	189	21.59	0.21	0.018
	37.38	201	23.8	0.24	0.018
	40.5	213	25.31	0.25	0.018
	41.58	225	25.72	0.26	0.018
	43.68	237	25.93	0.26	0.018
	45.72	249	25.9	0.26	0.018
	46.8	261	25.44	0.25	0.018
	49.98	273	26.83	0.27	0.018
	54.18	285	25.53	0.26	0.018
	56.22	297	26.6	0.27	0.018
	58.26	309	25.89	0.26	0.018
	62.4	321	24.61	0.25	0.018
	65.4	333	23.43	0.23	0.018
	66.6	345	22.9	0.23	0.018
	69	357	21.82	0.22	0.018
	75	369	19.23	0.2	0.018
	80.4	381	16.97	0.17	0.018
	81.6	393	16.6	0.17	0.018

Reference	E (keV)	$\pm \Delta E_{CM}$		$\pm \Delta S_{stat}$	Systematic uncertainty
		(eV)	S (MeV.b)	(MeV.b)	
	85.8	405	14.96	0.15	0.018
	87.6	417	14.27	0.14	0.018
	91.8	429	12.9	0.13	0.018
	93.6	441	12.33	0.12	0.018
	97.2	453	11.02	0.11	0.018
	100.2	465	10.63	0.11	0.018
	103.8	477	9.91	0.1	0.018
	109.8	489	8.99	0.09	0.018
	123	501	6.79	0.07	0.018
	136.2	513	5.44	0.05	0.018
	150.6	526	4.43	0.04	0.018
	165.6	540	3.55	0.04	0.018
	181.2	553	2.89	0.03	0.018
	197.4	570	2.51	0.03	0.018
	214.2	600	2.16	0.02	0.018

**Appendix B. The Data calculated and used for the T(d,n)<sup>4</sup>He reaction rate diagram of Fig. 3.**

T (GK)	Reaction rate as 50 <sup>th</sup> percentile of PDF (cm <sup>3</sup> mol <sup>-1</sup> s <sup>-1</sup> )
0.001	1.999 × 10 <sup>-7</sup>
0.002	1.447 × 10 <sup>-3</sup>
0.003	1.050 × 10 <sup>-1</sup>
0.004	1.541 × 10 <sup>0</sup>
0.005	1.038 × 10 <sup>1</sup>
0.006	4.410 × 10 <sup>1</sup>
0.007	1.400 × 10 <sup>2</sup>
0.008	3.619 × 10 <sup>2</sup>
0.009	8.071 × 10 <sup>2</sup>
0.010	1.618 × 10 <sup>3</sup>
0.011	2.940 × 10 <sup>3</sup>
0.012	4.999 × 10 <sup>3</sup>
0.013	8.054 × 10 <sup>3</sup>
0.014	1.244 × 10 <sup>4</sup>
0.015	1.835 × 10 <sup>4</sup>
0.016	2.615 × 10 <sup>4</sup>
0.017	3.500 × 10 <sup>4</sup>
0.018	4.995 × 10 <sup>4</sup>
0.020	8.420 × 10 <sup>4</sup>
0.025	2.502 × 10 <sup>5</sup>
0.030	5.746 × 10 <sup>5</sup>
0.040	1.950 × 10 <sup>6</sup>

T (GK)	Reaction rate as 50 <sup>th</sup> percentile of PDF ( $\text{cm}^3\text{mol}^{-1}\text{s}^{-1}$ )
0.050	$4.641 \times 10^6$
0.060	$9.016 \times 10^6$
0.070	$1.533 \times 10^7$
0.080	$2.351 \times 10^7$
0.090	$3.362 \times 10^7$
0.100	$4.540 \times 10^7$
0.110	$5.880 \times 10^7$
0.120	$7.333 \times 10^7$
0.130	$8.880 \times 10^7$
0.140	$1.060 \times 10^8$
0.150	$1.220 \times 10^8$
0.160	$1.392 \times 10^8$
0.170	$1.551 \times 10^8$
0.180	$1.735 \times 10^8$
0.190	$1.893 \times 10^8$
0.200	$2.077 \times 10^8$
0.250	$2.850 \times 10^8$
0.300	$3.500 \times 10^8$
0.350	$4.002 \times 10^8$
0.400	$4.380 \times 10^8$
0.450	$4.700 \times 10^8$
0.500	$4.881 \times 10^8$
0.600	$5.122 \times 10^8$
0.700	$5.215 \times 10^8$
0.800	$5.212 \times 10^8$
0.900	$5.160 \times 10^8$
1.000	$5.071 \times 10^8$